Available online at www.sciencedirect.com
SCIENCE DIRECT
Polymer 47 (2006) 3636–3649
polymer
www.elsevier.com/locate/polymer

Time-resolved SAXS studies on ordering kinetics of block copolymers: Further investigation of two-step ordering from disorder-sphere to hex-cylinder

Norihiro Sota [1], Naoki Sakamoto [2], Kenji Saijo, Takeji Hashimoto [3,*]

Department of Polymer Chemistry, Graduate School of Engineering, Kyoto University, Kyoto 615-8510, Japan

Received 25 August 2005; received in revised form 18 January 2006; accepted 6 March 2006

Abstract

We have conducted the systematical investigations for the ordering process and kinetics of both hexagonally packed cylindrical microdomains (hex-cylinder) and spheres in a body-centered cubic lattice (bcc-sphere) from spherical microdomains with a short-range liquid-like order (disorder-sphere) over a wide range of quench depth for a polystyrene-*block*-polyisoprene-*block*-polystyrene triblock copolymer, having order–order transition (OOT) temperature, T_{OOT}, at 190 °C between hex-cylinder and bcc-sphere, by using time-resolved small-angle X-ray scattering. As a result, we clearly assessed a range of temperature over which the two-step ordering from disorder-sphere to hex-cylinder occurs. A possible interpretation for the two-step ordering process was proposed in the text. The following three kinds of ordering processes are observed. (i) The single-step ordering of hex-cylinder: when the system is quenched into the temperature below 183.2 °C, hex-cylinder is directly transformed from disorder-sphere via the nucleation and growth process. The incubation time for the nucleation and the transition rate largely depend on the quench depth. (ii) The ordering of bcc-sphere: when the system is quenched into the temperature above 190 °C in the bcc-sphere phase, bcc-sphere is formed from disorder-sphere via the nucleation and growth process. The quench-depth dependence of the incubation time is very small, compared with that for hex-cylinder, and the transition rate is independent of the quench depth. (iii) The two-step ordering of hex-cylinder: when the system is quenched into the temperature range from 183.2 to 190 °C, the volume-filling metastable bcc-sphere is first developed by nucleation and growth, followed by the OOT from metastable bcc-sphere to hex-cylinder via the nucleation and growth process. The incubation time for the formation of metastable bcc-sphere is very close to that for the formation of equilibrium bcc-sphere, and the transition rate for the formation of metastable bcc-sphere is independent of the quench depth. Thus, the ordering pathways for the volume-filling of metastable bcc-sphere are almost identical to that for the volume-filling equilibrium bcc-sphere. The incubation time for the OOT from metastable bcc-sphere to hex-cylinder is longer than that for the formation of metastable bcc-sphere, and the transition rate for the former is also slower than that for the latter. Moreover, the incubation time for the OOT from metastable bcc-sphere to hex-cylinder is longer than that for that from equilibrium bcc-sphere to hex-cylinder, and the transition rate for the former is also slower than that for the latter, because metastable bcc-sphere is considered to be more distorted than the equilibrium bcc-sphere, which suppress the epitaxial growth of hex-cylinder along a [111] direction of bcc-sphere.

Keywords: Block copolymer; Ordering kinetics; Metastable bcc-sphere

1. Introduction

Now that the equilibrium phase behavior of block copolymers composed of two components is well understood [1–9], it becomes more and more important to understand the way how we control their patterns with nano-periodicity not only for a scientific interest but also for advanced practical applications. For this purpose, it is crucial to illuminate the process and kinetics of the phase transitions of the block copolymers. Unfortunately, they are not sufficiently studied at present. In this paper, we focus on elucidation of the two-step ordering process of hexagonally packed cylindrical

* Corresponding author. Tel.: +81 29 284 3833; fax: +81 29 282 5939.
E-mail address: hashimoto.takeji@jaea.go.jp (T. Hashimoto).
[1] Present address: BASF Aktiengeshellschaft, GKP/P-G200, D-67056 Ludwigshafen, Germany.
[2] Present address: Computer Science Department, Asahi Chemical Industry Co., Ltd, 2-1, Samejima, Fuji, Shizuoka 416-8501, Japan.
[3] Present address: Advanced Science Research Center, Japan Atomic Energy Agency, Tokai, Ibaraki 319-1195, Japan.

0032-3861/$ - see front matter © 2006 Elsevier Ltd. All rights reserved.
doi:10.1016/j.polymer.2006.03.017

microdomains (hex-cylinder) from spherical microdomains with a short-range liquid-like order (disorder-sphere) [10]. For this purpose, we systematically explored the ordering processes and kinetics of both hex-cylinder and spherical microdomains in a body-centered cubic lattice (bcc-sphere) from disorder-sphere as a function of quench depth by using the same asymmetric polystyrene-*block*-polyisoprene-*block*-polystyrene (SIS) triblock copolymer as previously employed [10–12], and by using time-resolved small-angle X-ray scattering (SAXS).

As shown in Fig. 1, the SIS triblock copolymer we employed in this study is well known to exhibit the order–order transition (OOT) between hex-cylinder and bcc-sphere at an OOT temperature, T_{OOT}, and the lattice disordering/ordering transition (LDOT), which is regarded as order-disorder phase transition in the context of the current theory, between disorder-sphere and bcc-sphere at a LDOT temperature, T_{LDOT} [10–12]. By using this triblock copolymer, Sakamoto and Hashimoto have explored the nucleation and growth processes for the ordering of hex-cylinder induced by the temperature quench from T_{LDOT}, ΔT_{LDOT} ($\equiv T_{LDOT} - T_{hex}$) = 40 K and for that of bcc-sphere induced by ΔT_{LDOT} ($\equiv T_{LDOT} - T_{bcc}$) = 18 K [12]. A similar work was also reported by Kim et al. on the same block copolymer [13]. Here, T_{hex} and T_{bcc} are targeted temperatures where the isothermal ordering of hex-cylinder and bcc-sphere take place, respectively. Indeed, the ordering processes of hex-cylinder and bcc-sphere have been elucidated at the given ΔT_{LDOT}s. However, systematic studies on the ordering process of hex-cylinder and bcc-sphere as a function of ΔT_{LDOT} have not been explored yet, even though the triblock copolymer has such a merit that the ordering processes of the two different microdomain structures can be explored with the same sample and can be compared with each other. Therefore, we aim to study systematically the isothermal ordering kinetics and process as a function of temperature across T_{OOT} and T_{LDOT} in this paper.

In the ordering of hex-cylinder from disorder-sphere, the system is quenched across T_{LDOT} and T_{OOT}. Recently, we have found that there are two kinds of the ordering process of hex-cylinder starting from disorder-sphere, depending on the quench depth from T_{OOT}, ΔT_{OOT} ($\equiv T_{OOT} - T_{hex}$) [10]. When the system is deeply quenched into the temperature below T_{OOT} (ΔT_{OOT} = 10 K or ΔT_{LDOT} = 40 K), hex-cylinder is directly formed from disorder-sphere via the nucleation and growth process. Hereafter, this ordering of hex-cylinder is designated as the single-step ordering of hex-cylinder. However, when the system is shallowly quenched into the temperature below T_{OOT} (ΔT_{OOT} = 2.5 K or ΔT_{LDOT} = 32.5 K), the volume-filling metastable bcc-sphere is first developed by nucleation and growth, followed by the OOT into equilibrium hex-cylinder (via the nucleation and growth). Hereafter, this striking ordering process of hex-cylinder is referred to the two-step ordering of hex-cylinder. However, we have not yet elucidated a range of temperature over which this intriguing two-step ordering occurs. Therefore, in this paper, we aim to elucidate this temperature range as well by means of time-resolved SAXS as a function of temperature.

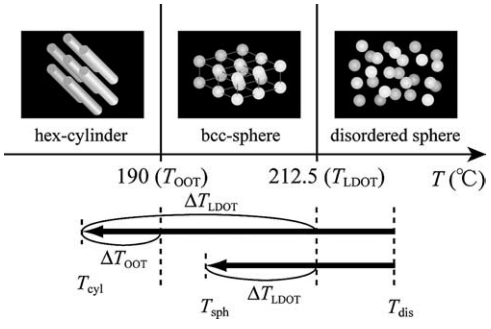

Fig. 1. Schematic illustration of the phase behavior for the SIS triblock copolymer and of T-drop experiments from disorder-sphere to bcc-sphere or to hex-cylinder. Definitions of ΔT_{LDOT} and ΔT_{OOT} are also shown.

It is important to note the following point in the discussion of the two-step ordering process. The OOT between bcc-sphere and hex-cylinder occurs in the temperature region between 188 °C (below which hex-cylinder exists) and 193 °C (above which bcc-sphere exists) by using the SAXS data taken as a function of temperature with a narrow temperature increment across the OOT. The OOT temperature was defined 190 °C in this paper. Thus, the temperature corresponding to the shallow quench of ΔT_{OOT} = 3 and 4 K (187 and 186 °C), is definitely that inside the hex-cylinder phase. The case of ΔT_{OOT} = 2 K appears to be marginal. However, at the long time limit, as long as 10^5 s, of the isothermal ordering process, the SAXS profile (as shown in Fig. 4 later in this work for ΔT_{OOT} = 3 K) and the TEM image (as shown in Fig. 6(d) in Ref. [10] for ΔT_{OOT} = 2.5 K) definitely reveal that the equilibrium morphology is hex-cylinder at ΔT_{OOT} = 2 K. The same is applied for the cases of ΔT_{OOT} = 3 and 4 K.

The systematic studies enable us to compare the ordering kinetics from disorder-sphere to the following states as well: (i) hex-cylinder in the single-step ordering process ((a-1) in Scheme 1), (ii) the volume-filling metastable bcc-sphere in the two-step ordering process ((a-2) in Scheme 1) and (iii) equilibrium bcc-sphere ((a-3) in Scheme 1). Furthermore, they allow us to compare the OOT kinetics from the volume-filling metastable bcc-sphere to hex-cylinder in the two-step ordering process ((a-2′) in Scheme 1) and that from equilibrium bcc-sphere to hex-cylinder ((b) in Scheme 1) [14], as will be discussed in the end of this paper.

2. Experimental method

We use the SIS triblock copolymer (Vector4111, Dexco Polymers Company) in this study. The sample and the method of preparing it are basically the same as we employed before in the companion paper [10]. Hence, only the brief description is given in this paper. The characteristics of this sample are as follows: (i) the weight-averaged molecular weight, M_w; 1.4×10^5, (ii) the polydispersity index, M_w/M_n (M_n is the number-averaged molecular weight); 1.11, (iii) the weight fraction of polystyrene; 0.183. The sample was dissolved into toluene with a small amount of antioxidant (Irganox 1010, Ciba-Geigy Group) and cast into film specimen from a 10 wt% solution by

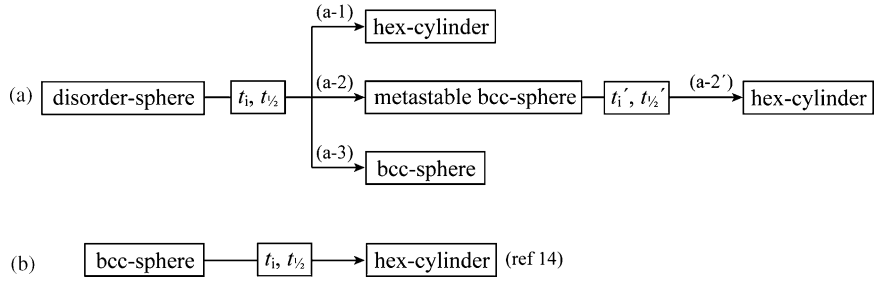

Scheme 1. Ordering processes and kinetics as studied in this work, (a) and in Ref. [14], (b).

evaporating the solvent slowly in a fume hood for 1 week. The phase transition temperatures, T_{OOT} and T_{LDOT}, of the film specimen were reassessed to be 190 and 212.5 °C, respectively, by the temperature change of the peak intensity and Bragg spacing obtained from the static SAXS experiments in the heating cycle from 175 to 230 °C. These T_{OOT} and T_{LDOT} are slightly different from those described in the previous works [10,12] because the film specimen for this study are prepared newly and differ from those used previously.

The experimental methods are also almost the same as we employed before in the companion paper [10]. We will describe them in brief here. The ordering process from disorder-sphere to hex-cylinder or to bcc-sphere was induced by a temperature drop (T-drop). In investigating the ordering processes of hex-cylinder, the T-drop experiments were conducted by quenching from 227 °C, where disorder-sphere exists at equilibrium, to $T_{hex}=175$, 179, 183, 186, 187 and 188, where hex-cylinder exists at equilibrium, i.e. $\Delta T_{LDOT}=37.5$, 33.5, 29.5, 26.5, 25.5 and 24.5 K or $\Delta T_{OOT}=15$, 11, 7, 4, 3 and 2 K, respectively. While, in exploring the ordering processes of bcc-sphere, the T-drop experiments were conducted by quenching from 227 °C to $T_{bcc}=193$, 199 and 203, where bcc-sphere exists at equilibrium, i.e. $\Delta T_{LDOT}=19.5$, 13.5 and 9.5 K, respectively. After 10 min anneal of the specimen at 227 °C followed by T-drops, the thermally induced ordering processes were observed by time-resolved SAXS. Here, the starting time was set zero at the time when the specimen reached a targeted temperature.

The SAXS apparatus consists of an 18-kW rotating-anode X-ray generator (SRAM18XH MAC Science Co. Ltd) with a graphite crystal monochromator to obtain Cu Kα beam (wavelength: 0.154 nm) and a vacuum chamber for both the incident-beam path and scattered beam path. It was used by the generator power of 12 kW (40 kW and 300 mA). As a detector, one-dimensional position sensitive proportional counter (PSPC) with line focus optics was used. The SAXS profiles were measured with varying exposure time to incident X-ray beam in the range of 60–3000 s and corrected for the absorption of the sample, air scattering and slit-height and slit-width smearing [15–17], unless otherwise stated. The absolute SAXS intensity was obtained by using the nickel-foil method [18].

In addition, TEM observation for the specimen frozen at particular times of the ordering process was also conducted. The same freezing method was used as that reported in the previous works [10,12,19,20]. We confirmed that the freezing of the specimen was successful by checking effectively no changes of SAXS profiles before and after freezing. The ultrathin sections of ca. 50 nm thickness were microtomed under −100 °C by a Reichert Ultracut S with the cryochamber FCS and a diamond knife (DiATOME, Switzerland), and were picked up on a 400 mesh copper grid. After staining the specimen by the vapor of 2% aqueous solution of osmium tetraoxide (O_sO_4) for 1 h at room temperature to stain selectively polyisoprene (PI) domains, they were observed by a TEM (JEOL JEM-2000FXZ) operated with 120 kV.

3. Experimental results

3.1. Single-step ordering processes from disorder-sphere to hex-cylinder or to bcc-sphere

Fig. 2 shows typical time evolutions of the SAXS profiles after T-drop from 227 °C to (a) 183 °C ($\Delta T_{LDOT}=29.5$ K, $\Delta T_{OOT}=7$ K) and to (b) 193 °C ($\Delta T_{LDOT}=19.5$ K), plotted as a function of the scattering vector, q, defined by $q=(4\pi/\lambda)\sin(\theta/2)$ with λ and θ being the wavelength of the incident X-ray and the scattering angle, respectively. We deliberately show the profiles without silt corrections to prevent any artifacts that might be induced by the corrections. In Fig. 2(a), the SAXS profiles right after T-drop have a broad second-order shoulder at $q=0.35$ nm^{-1}, marked by the thick arrow. They do not change for ca. 2000 s after T-drop. After this period, the higher-order peaks at $q=\sqrt{3}q_m$ and $\sqrt{4}q_m$, where q_m is the wave vector at the first-order peak, appear and are becoming higher and sharper with time. Therefore, it is found that the period when the SAXS profiles are identical is the incubation period for the ordering process where the system stays at a disorder-sphere state. Then, the ordering of hex-cylinder proceeds directly from disorder-sphere via the nucleation and growth process. Thus, the system is concluded to select the single-step ordering of hex-cylinder at $\Delta T_{LDOT}=29.5$ K or $\Delta T_{OOT}=7$ K. While, in Fig. 2(b), the SAXS profiles right after T-drop have also the broad second-order shoulder marked by the thick arrow and do not change for ca. 2500 s after T-drop. After this period, the higher-order peaks at $q=\sqrt{2}q_m$ and $\sqrt{3}q_m$ appear and become increasingly distinct with time. Therefore, at $\Delta T_{LDOT}=19.5$ K, the ordering of bcc-sphere is found to proceed via the nucleation and growth process after the incubation time.

Fig. 3(a) shows the time evolutions of the peak intensity, $I_m=I(q=q_m)$, obtained from the SAXS profiles, corrected for

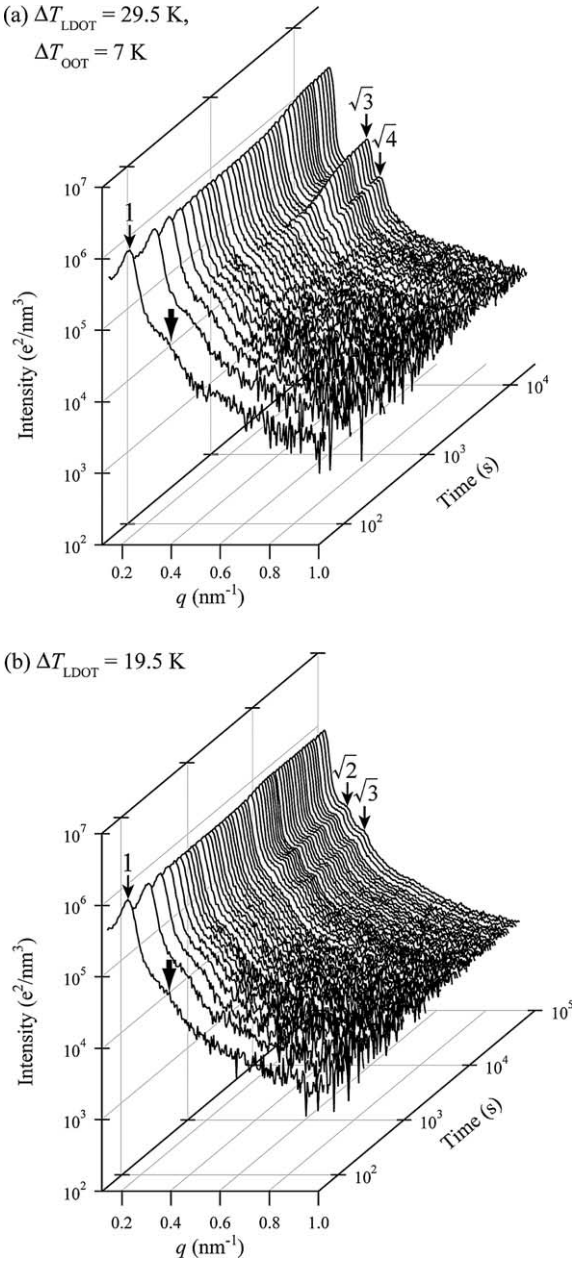

Fig. 2. Time evolutions of the SAXS profiles for the SIS triblock copolymer after T-drop from 227 °C to (a) 183 °C (ΔT_{LDOT} = 29.5 K, ΔT_{OOT} = 7 K) at which hex-cylinder exists at equilibrium and to (b) 193 °C (ΔT_{LDOT} = 19.5 K) at which bcc-sphere exists at equilibrium. The profiles without slit corrections are deliberately shown here to prevent any artifacts that might be induced by the slit corrections.

the slit smearings, in the ordering processes induced by the several T-drops to 175, 179, 183, 193, 199 and 203 °C (ΔT_{LDOT} = 37.5, 33.5, 29.5, 19.5, 13.5 and 9.5 K), while, in Fig. 3(b), the curves in Fig. 3(a) are vertically shifted up by 1×10^6 relative to the one presented immediately below so as to avoid overlaps. The curve numbered as (6) indicates the actual value. In all the ordering processes at various ΔT_{LDOT}, I_m stays at a constant value for a certain incubation period and then starts to increase. This proves that all the ordering processes proceed via the nucleation and growth process and reflects

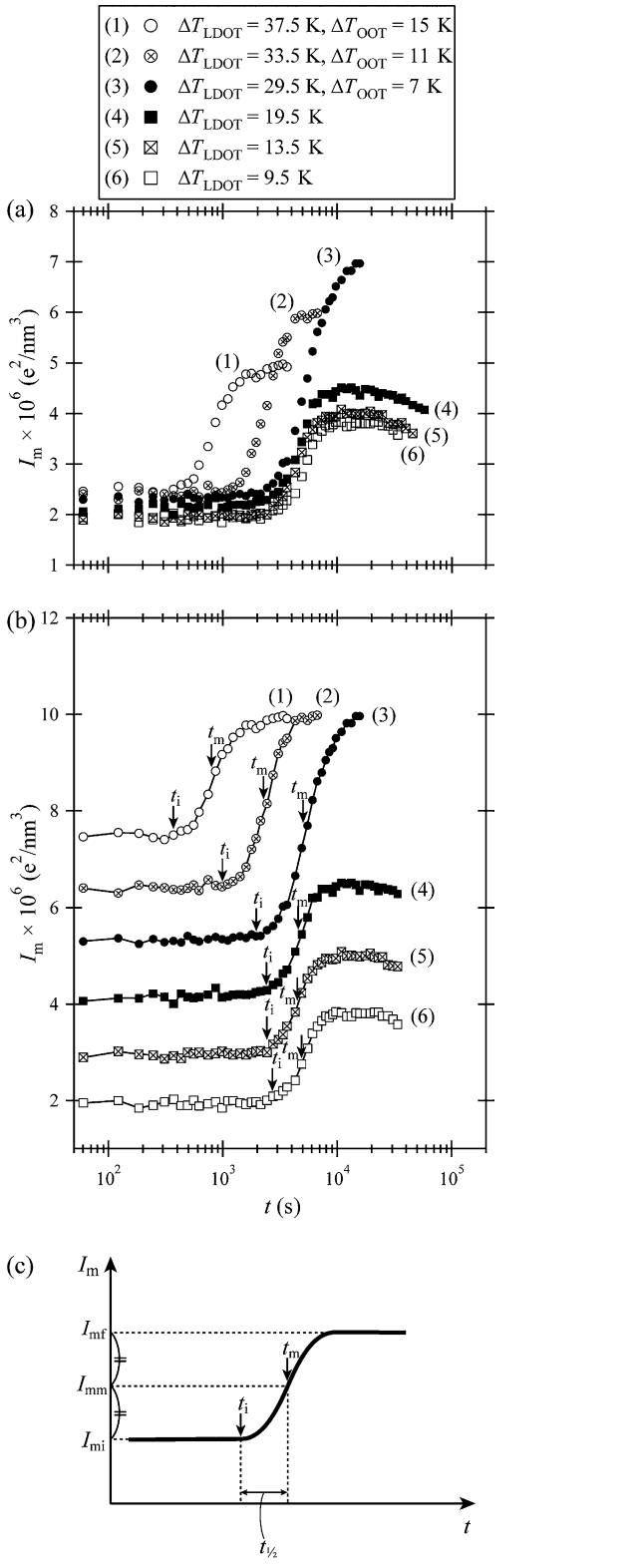

Fig. 3. (a) Time evolutions of the peak intensity, I_m, obtained from the desmeared SAXS profile for the SIS triblock copolymer after T-drop from 227 °C to 175, 179, 183, 193, 199 and 203 °C (ΔT_{LDOT} = 37.5, 33.5, 29.5, 19.5, 13.5 and 9.5 K, corresponding to the curves (1)–(6), respectively). The curves in (b) are shifted up by 1×10^6 relative to the one immediately below in order to avoid overlaps of the curves (1)–(6) in (a). The curve numbered as (6) indicates the actual intensity value. The curves (1)–(3) represent the single-step ordering processes from disorder-sphere to hex-cylinder, while those (4)–(6) represent

the first-order phase transition. From the curves (1)–(3) in this figure together with the time evolutions of the SAXS profiles as shown in Fig. 2(a), we found the normal ordering into hex-cylinder, i.e. the single-step ordering into hex-cylinder at $\Delta T_{LDOT}=37.5$, 33.5 and 29.5 K, while the ordering into bcc-sphere occurs at $\Delta T_{LDOT}=19.5$, 13.5 and 9.5 K (curves (4)–(6)). In the ordering processes of hex-cylinder, the larger ΔT_{LDOT} is, the faster the ordering proceeds. Therefore, the incubation time, t_i, defined in Fig. 3(c) together with t_m, becomes shorter. On the other hand, the incubation time and the time changes of I_m hardly change in the ordering processes of bcc-sphere. t_i is defined as the time (shown by the arrow in Fig. 3(b)) when I_m starts to increase from the intensity level, I_{mi}, in the incubation time. While $t_{1/2}$ is defined as follows: t_m is the time (shown by the arrow in Fig. 3(b)) where I_m reaches I_{mm} defined by $(I_{mi}+I_{mf})/2$, with I_{mf} being the intensity level in the late stage of the ordering process. Then, $t_{1/2}$ is defined as t_m-t_i. Hence, t_i and t_m in the I_m curves of these ordering processes are assessed as indicated by the arrows in Fig. 3(b).

3.2. Ordering processes of hex-cylinder induced by shallow quenches, $\Delta T_{OOT}=4$, 3 and 2 K

Fig. 4 shows the time evolution of the SAXS profiles after T-drop from 227 to 187 °C ($\Delta T_{LDOT}=25.5$ K, $\Delta T_{OOT}=3$ K), plotted as a function of q. We deliberately show again the profiles without silt corrections to prevent any artifacts that might be induced by the corrections here, too. The nine SAXS profiles selected from Fig. 4(a) are shown in Fig. 4(b). Here, the intensities of the profile ① are actual values, and the intensities of the other profiles are shifted down vertically by one decade relative to the intensities immediately above in order to avoid overlaps. The SAXS profiles right after T-drop have a broad second-order shoulder at $q=0.35$ nm^{-1}, marked by the thick arrow in the profiles ① and ②. They do not change for ca. 2500 s after T-drop. After this period, the higher-order peaks can be first seen at $q=\sqrt{2}q_m$ and $\sqrt{3}q_m$, even though the specimen is quenched into the temperature where hex-cylinder exists at equilibrium (see the profiles ③ to ⑤). From around 10,000 s after T-drop, the higher-order peaks at $q=\sqrt{3}q_m$ and $\sqrt{4}q_m$ are becoming higher and sharper, while that at $q=\sqrt{2}q_m$ starts to decrease its intensity and eventually disappears (see the profiles ⑥ to ⑨). This result indicates that bcc-sphere is first formed transiently from disorder-sphere via the nucleation and growth process and then transformed into equilibrium hex-cylinder. That is, the two-step ordering of hex-cylinder occurs at $\Delta T_{LDOT}=25.5$ K or $\Delta T_{OOT}=3$ K.

Fig. 5 shows the time evolutions of I_m obtained from the SAXS profiles corrected for the slit smearings in the ordering processes of hex-cylinder induced by the shallow quenches. In part (a), time evolutions of I_m for the single-step ordering of hex-cylinder and the ordering of bcc-sphere are also shown by the gray symbols for the sake of comparison. In Fig. 5(b), the curves which indicate the time evolutions of I_m only for the shallow quench are shifted up by 1×10^6 relative to the one presented immediately below so as to avoid overlaps.

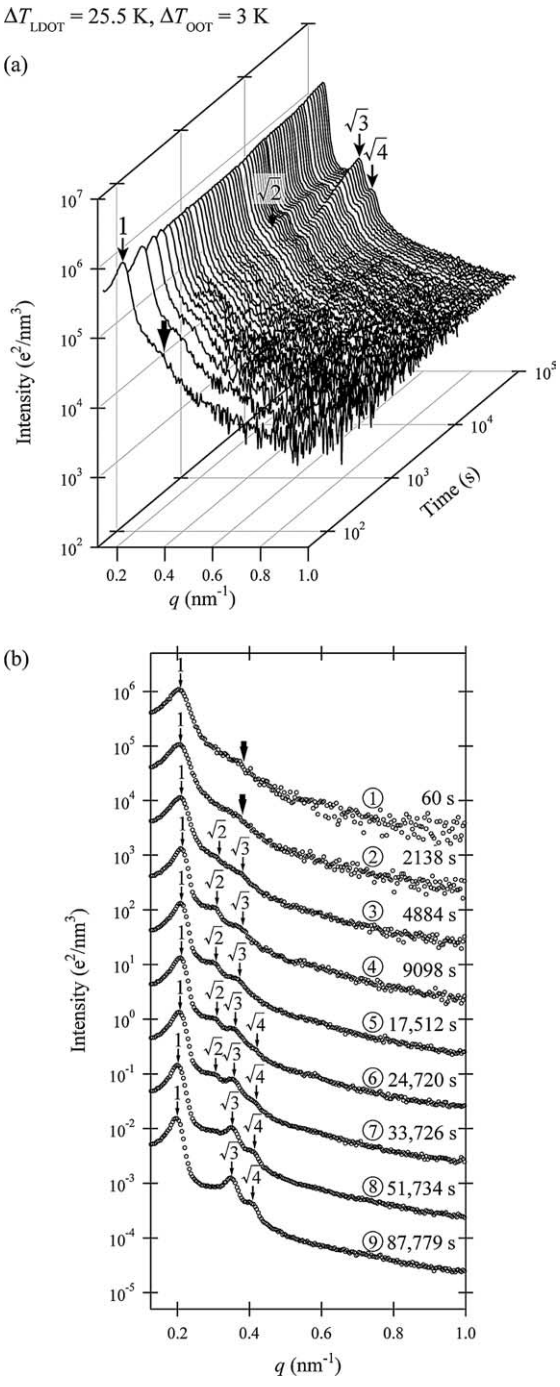

Fig. 4. Time evolutions of the SAXS profiles for the SIS triblock copolymer after T-drop from 227 to 187 °C ($\Delta T_{LDOT}=25.5$ K, $\Delta T_{OOT}=3$ K), where hex-cylinder exists at equilibrium. The profiles without slit corrections are deliberately shown here to prevent any artifacts that might be induced by the slit corrections. The nine SAXS profiles during this ordering process selected from (a) are shown in (b) with a vertical shift to avoid an overlap of the profiles. The intensities of the profile ① are actual values, and the intensities of the other profiles are shifted down vertically by one decade relative to the intensities immediately above.

the ordering processes from disorder-sphere to bcc-sphere. (c) Definitions of an incubation time, t_i, a time, t_m, and a half time, $t_{1/2}=t_m-t_i$, in the time evolution of I_m. On the basis of (c), t_i and t_m are assessed for each curve as indicated by the arrows in (b).

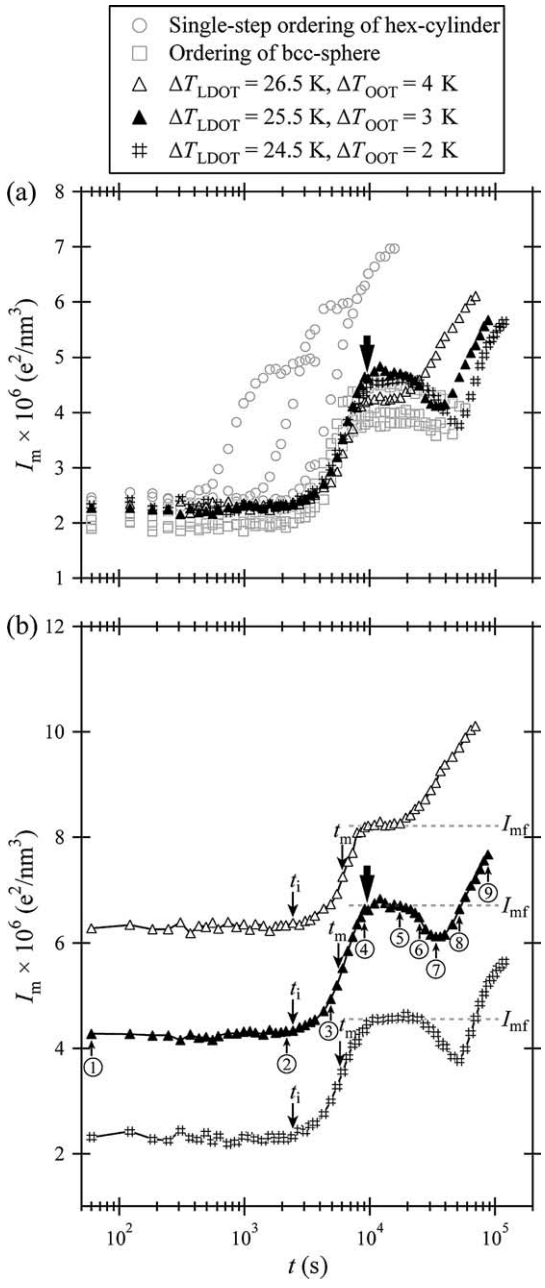

Fig. 5. Time evolutions of the peak intensity, I_m, obtained from the desmeared SAXS profiles, shown by the dark symbols, for the SIS triblock copolymer after T-drop from 227 °C to 186, 187 and 188 °C (ΔT_{LDOT}=26.5, 25.5 and 24.5 K or ΔT_{OOT}=4, 3 and 2 K). The time evolutions of I_m for the single-step ordering into hex-cylinder and into bcc-sphere (i.e. the same data as shown in Fig. 5(a)) are also shown by the gray symbols for comparison in (a). The specimen is frozen for the TEM observation at the time shown by the thick arrow in (a) and (b). The curves in (b) are shifted up by 1×10^6 relative to the one immediately below in order to avoid overlaps in (a). The curve shown at the bottom of (b) indicates the actual value. The arrows with the numbers in circles for the I_m curve obtained for ΔT_{OOT}=3 indicate the time when the nine SAXS profiles in Fig. 4(b) are measured. On the basis of Fig. 3(c), t_i and t_m are assessed as indicated by the arrows in (b), where I_{mf} is the intensity level indicated by the broken gray line in this case.

The curve shown at the bottom of this figure indicates the actual value. The arrows with the numbers in circles for the I_m curve of ΔT_{OOT}=3 indicate the time when the nine SAXS profiles in Fig. 4(b) are measured. I_m is constant for a certain incubation period, t_i, and then starts to increase, so that these ordering processes also proceed via the nucleation and growth process. The higher-order peaks at $q=\sqrt{2}q_m$ and $\sqrt{3}q_m$ start to appear after the incubation time, so that bcc-sphere rather than hex-cylinder is first formed from disorder-sphere in these ordering processes despite of the fact that the system is quenched into the temperature where hex-cylinder exist at equilibrium. Then, I_m stops increasing at around 10,000 s after T-drop and stays at a certain value for a certain period. Here, this intensity level in the period is defined as I_{mf} in these ordering processes as indicated by the gray dotted lines in Fig. 5(b). Then, t_i and t_m in the I_m curves are assessed as indicated by the arrows in Fig. 5(b), as defined in Fig. 3(c).

The higher-order peaks at $q=\sqrt{2}q_m$ and $\sqrt{3}q_m$ can be clearly seen as shown in the profiles ④ and ⑤ in Fig. 4(b) during this period. In addition, the TEM observation is conducted to investigate the transient structure at that time. As a representative, Fig. 6 shows the TEM image for the specimen frozen at 9700 s after T-drop to 187 °C (ΔT_{OOT}=3 K), indicated by the thick arrow in Fig. 5. The bright PS spherical microdomains packed hexagonally could be seen. An observation of the image over a wide area indicated that bcc-sphere is volume-filling at this time. The image is considered to be viewed along a [111] direction of bcc-sphere. Then, metastable bcc-sphere is transformed into equilibrium hex-cylinder. Thus, the two-step ordering of hex-cylinder occurs at ΔT_{OOT}=4, 3 and 2 K. Interestingly enough, the incubation time and the time change of I_m in these ordering processes hardly depend on ΔT_{OOT} until the system reaches the volume-filling of bcc-sphere.

Now, the time evolutions of I_m, the square of the half-width at half maximum, σ_q^2, and Bragg spacing, $D=2\pi/q_m$, are shown in Fig. 7 to explore these ordering processes in detail. The arrows with the numbers in circles and the gray broken line pointed by those arrows indicate the time when the SAXS profiles of ΔT_{OOT}=3 K in Fig. 4(b) are measured. We are specially concerned with the behaviors of I_m, σ_q^2 and D in the time region after the time ④ in the figure. I_m hardly changes for a certain time after ca. 10,000 s (point ④ in Fig. 7) and before ca. 18,000 s (point ⑤ in Fig. 7). Then, it slightly decreases and increases for ΔT_{OOT}=2 and 3 K, though it continuously keeps increasing without the decrease for ΔT_{OOT}=4 K. On the contrary, σ_q^2 indicates a constant value for a certain period, then increases to a maximum value and eventually turns to a decrease. The trend looks almost the same for ΔT_{OOT}=2, 3 and 4 K, though the time period where σ_q^2 is constant is short and the maximum is very broad for ΔT_{OOT}=4 K. On the other hand, D gradually increases just a little for a certain time after ca. 10,000 s and then increases rapidly. The reason why these three parameters changes as described above will be discussed in Section 4.2.

Before closing this section, we like to note the following remark. As already elucidated, the OOT process involves the nucleation and growth of the metastable bcc-sphere phase in the matrix of the disorder-sphere phase (the first step) and the nucleation and growth of the hex-cylinder phase in the matrix of the volume-filling metastable bcc-sphere phase (the second step) [10]. In each step, the former phase grows at the expense

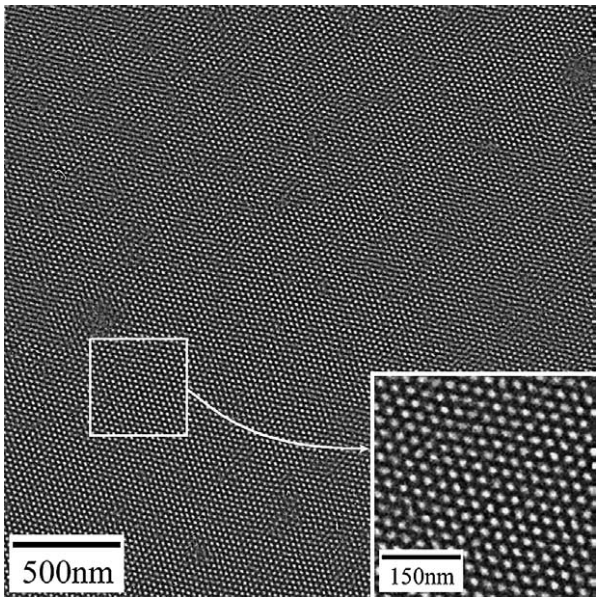

Fig. 6. Transmission electron microscope image for the SIS triblock copolymer frozen at 9700 s (corresponding to the point indicated by the thick arrow in Fig. 5, where the volume-filling metastable bcc-sphere are formed) after T-drop to 187 °C ($\Delta T_{LDOT}=25.5$ K, $\Delta T_{OOT}=3$ K). The inset enlarges the region encompassed by the white square.

of the latter phase. The first-order scattering maximum of the disorder-sphere phase locates close enough to that of the metastable bcc-sphere phase, so that they overlap into a broad scattering maximum. The same phenomenon is also noticed for the transition between the metastable bcc-sphere phase and the equilibrium hex-cylinder phase. Therefore, the characteristic scattering parameters for the net first-order scattering maximum changes continuously with time during the transition processes, as elucidated elsewhere [14] for the OOT from the equilibrium bcc-sphere phase to the equilibrium hex-cylinder phase.

4. Discussion

4.1. Quench-depth dependence of ordering processes for the SIS triblock copolymer

The experimental results have led us to classify the ordering processes of the SIS triblock copolymer into the three kinds; the single-step ordering of hex-cylinder, the two-step ordering of hex-cylinder, and the (single-step) ordering of bcc-sphere. We would like to first discuss ΔT_{LDOT} dependence of t_i in the ordering processes, as shown in Fig. 8(a), to illuminate the ordering kinetics. The data points of t_i for the single-step ordering of hex-cylinder from disorder-sphere, the ordering of bcc-sphere from disorder-sphere, and the two-step ordering of hex-cylinder from disorder-sphere, assessed in Figs. 3(b) and 5(b), are marked by circles, squares and triangles, respectively. A black solid line and a gray one are obtained by the least square fitting of the data points for the single-step ordering of hex-cylinder and the ordering of bcc-sphere, respectively, and are expressed as follows:

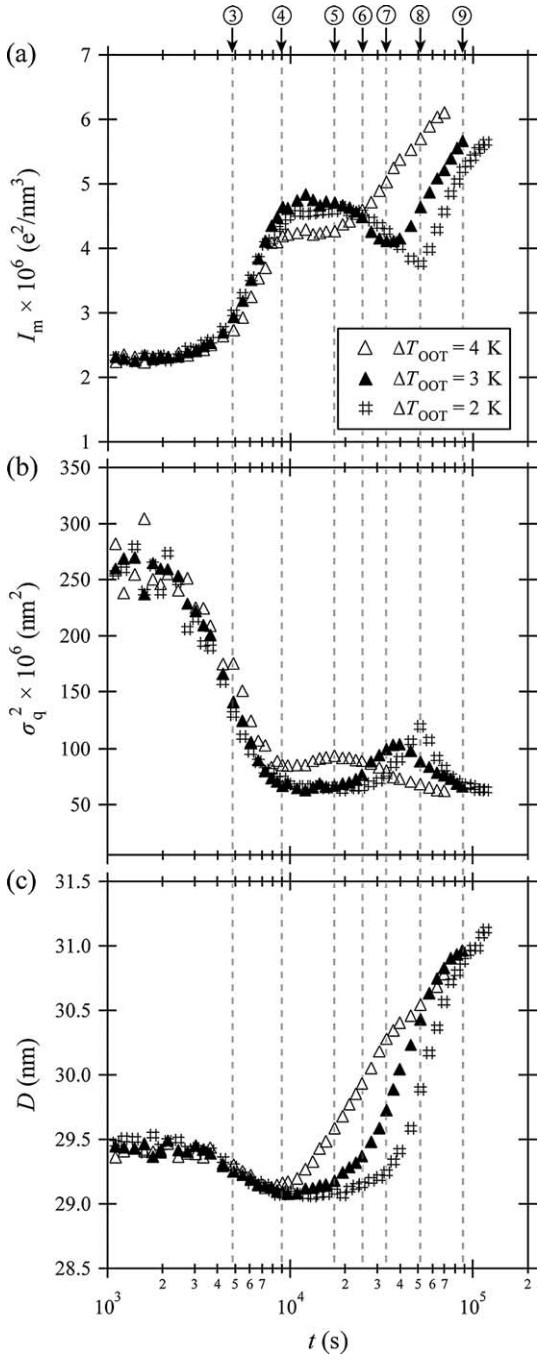

Fig. 7. Time evolutions of (a) the peak intensity, I_m, (b) the square of the half-width at half maximum, σ_q^2, (c) the Bragg spacing, D, obtained from the desmeared SAXS profile for the SIS triblock copolymer after T-drop from 227 °C to 186, 187 and 188 °C ($\Delta T_{OOT}=4$, 3 and 2 K). The arrows with the numbers in circles and the gray broken vertical line pointed by those arrows indicate the time when the SAXS profiles of $\Delta T_{OOT}=3$ in Fig. 4(b) are measured.

$$\log t_i = 5.98 - 0.0904\ \Delta T_{LDOT} \quad (1)$$

(Single-step ordering of hex-cylinder)

$$\log t_i = 3.47 - 0.00467\ \Delta T_{LDOT} \quad (2)$$

(Ordering of bcc-sphere)

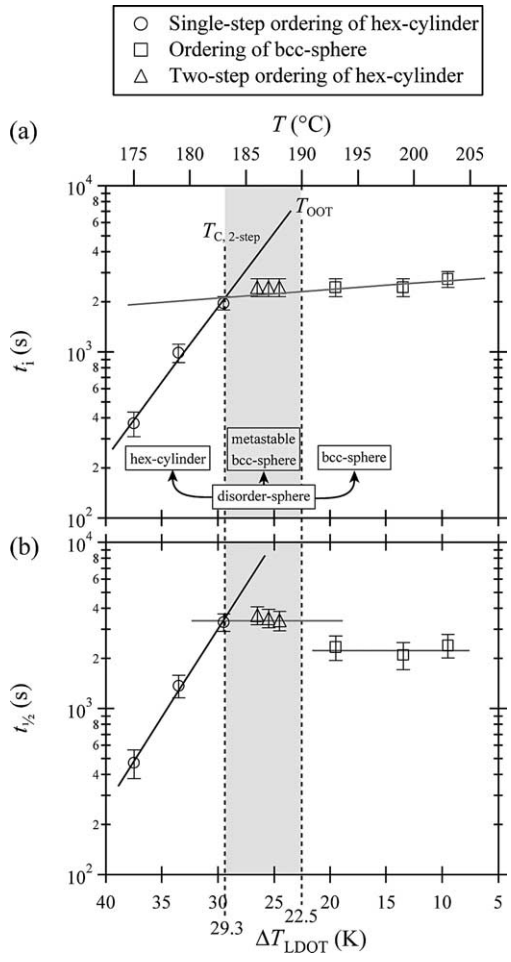

Fig. 8. ΔT_{LDOT} dependence of (a) the incubation time, t_i, and (b) the half time, $t_{1/2}$, in the ordering processes of the SIS triblock copolymer. Note that ΔT_{LDOT} increase from right to left. Circles, squares, and triangles indicate t_i for the single-step ordering processes of hex-cylinder (expressed as hex-cylinder), the ordering processes of equilibrium bcc-sphere (expressed as bcc-sphere) and the ordering process of metastable bcc-sphere (expressed as metastable bcc-sphere) in the two-step ordering processes of hex-cylinder, respectively. The black solid line and the grey one in (a) show the fitting line of t_i in the ordering processes of hex-cylinder and bcc-sphere, respectively. The black solid line in (b) shows the fitting line of $t_{1/2}$ for the single-step ordering processes of hex-cylinder, and the gray solid lines in (b) are drawn to indicate almost no ΔT_{LDOT} dependence for the ordering processes of equilibrium bcc-sphere and that of metastable bcc-sphere in the two-step ordering processes of hex-cylinder. The gray zone, i.e. the range of $22.5 \leq \Delta T_{LDOT} \leq 29.3$, shows that the two-step ordering of hex-cylinder occurs.

Interestingly and surprisingly also, we found the following experimental results: (i) the black line and the gray line are crossed at $\Delta T_{LDOT} = 29.3$ K or $\Delta T_{OOT} = 6.8$ K rather than at T_{OOT}; (ii) t_i's for formation of metastable bcc-sphere are on the same gray line drawn for t_i's for formation of equilibrium bcc-sphere. As a consequence, in the temperature gap between T_{OOT} and the crossing point between the two straight lines, defined as $T_{c,2\text{-step}}$, which is shown by the gray zone in Fig. 8, the system selects a kinetic pathway of the two-step ordering process rather than that of the single-step ordering into hex-cylinder before attaining equilibrium hex-cylinder.

Next, we would like to discuss significance and interpretation of our results on the two-step ordering process. The incubation time may be associated with the free energy barrier, Δf^*, for nucleation of the ordered grain in the matrix of disorder-sphere. Then, the black line and the gray line are related to temperature dependence of Δf^* for hex-cylinder, Δf^*_{hex}, and for bcc-sphere, Δf^*_{bcc}. The larger temperature dependence of t_i for hex-cylinder than for bcc-sphere means that the temperature dependence of Δf^*_{hex} is larger than that of Δf^*_{bcc}. If Δf^*_{hex} is equal to Δf^*_{bcc} at T_{OOT}, then the two lines cross at T_{OOT} as shown schematically in Fig. 8(a). If this is the case, the ordering process from disorder-sphere to hex-cylinder involves only the single-step ordering process (Fig. 9).

The fact that the two lines cross at $T_{c,2\text{-step}}$ lower than T_{OOT} as shown in Fig. 8(a) means that Δf^*_{hex} is larger than Δf^*_{bcc} at T_{OOT}. We note that Δf^* for the nucleation of the ordered grain is composed of the bulk free energy term, Δf^*_{bulk}, and the interfacial free energy term, Δf^*_{inter}, between the grain and the matrix. Furthermore, Δf^*_{bulk} for hex-cylinder and that for bcc-sphere are identical at T_{OOT}. Thus, the prediction of $\Delta f^*_{hex} > \Delta f^*_{bcc}$ at T_{OOT} suggests that Δf^*_{inter} for hex-cylinder, $\Delta f^*_{inter-hex}$, is greater than that for bcc-sphere, $\Delta f^*_{inter-bcc}$. Moreover, the fact that $\Delta f^*_{inter-hex} > \Delta f^*_{inter-bcc}$ is proposed to be due to a large conformational entropy loss of PI block chains between hex-cylinder and disorder-sphere at the grain interface as schematically illustrated in Fig. 10 of the previous companion paper [10]. As ΔT_{OOT} increases, the contribution of Δf^*_{inter} relative to that of Δf^*_{bulk} decreases, so that the difference between Δf^*_{hex} and Δf^*_{bcc} becomes less significant and negligible at $T_{c,2\text{-step}}$, as shown in Fig. 8(a).

$t_{1/2}$ is inversly related to the growth rate of hex-cylinder, metastable bcc-sphere, and equilibrium bcc-sphere after the incubation time. It is intriguing to note that the $t_{1/2}$ values for metastable bcc-sphere, $t_{1/2,meta\text{-}bcc}$, and those for equilibrium bcc-sphere, $t_{1/2,equ\text{-}bcc}$, are independent of temperature, as shown by the two gray lines in Fig. 8(b). It is even more intriguing to note that $t_{1/2,meta\text{-}bcc} > t_{1/2,equ\text{-}bcc}$, despite of the following two facts: (i) ΔT_{LDOT} is larger for the ordering of metastable bcc-sphere than that of equilibrium bcc-sphere; (ii) Temperature dependence of t_i's for metastable bcc-sphere and for equilibrium bcc-sphere fall on the same gray line as shown in Fig. 8(a). The slow growth rate of metastable bcc-sphere might reflect a tendency of system to form hex-cylinder from less ordered bcc-sphere or from bcc-sphere with an interface fluctuation between sphere and ellipsoid.

4.2. Two-step OOT processes: kinetics from metastable bcc-sphere to hex-cylinder

In this section, we would like to discuss the OOT processes and kinetics from metastable bcc-sphere to hex-cylinder in the two-step ordering of hex-cylinder. It should be noted that the OOT processes and kinetics from equilibrium bcc-sphere to hex-cylinder was reported elsewhere [14]. First, in Fig. 10, we show the time evolutions of the three characteristic parameters, I_m, σ_q^2 and D, magnified around the period when the volume-filled metastable bcc-sphere starts to undergo the OOT into hex-cylinder. We shall define two times, $t_{m\text{-}bcc}$ and t_s: $t_{m\text{-}bcc}$ is the time when the system reaches the volume-filled metastable

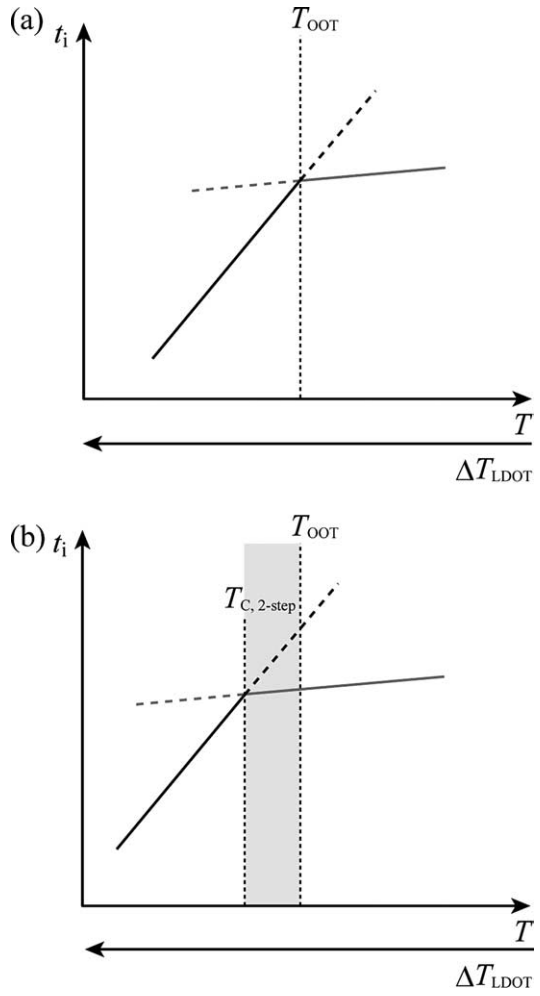

Fig. 9. Schematic illustrations of the possible ΔT_{LDOT} dependence of t_i (a) when the free energy barrier for the ordering from disorder-sphere to hex-cylinder is the same as that from disorder-sphere to bcc-sphere at T_{OOT} and (b) when the former is higher than the latter at T_{OOT}. The black line and the gray one indicate temperature dependence of t_i in the single-step ordering of hex-cylinder and the ordering of bcc-sphere, respectively. The gray zone in (b) indicates the temperature range where the two-step ordering of hex-cylinder occurs.

bcc-sphere; t_s is the time when the OOT from metastable bcc-sphere to hex-cylinder starts. $t_{m\text{-}bcc}$ is assessed as the time when I_m stops increasing and σ_q^2 and D stop decreasing. t_s is assessed as the time when I_m starts decreasing and σ_q^2 and D start increasing although the decrease of I. In the period from $t_{m\text{-}bcc}$ to t_s, each of the three parameters stays almost at a constant value, though D is slightly increasing. Moreover, the scaled structure factors obtained at various times during this period are universal with time, as shown in Fig. 11. Therefore, the symmetry of bcc-sphere is maintained, and bcc-sphere exists as a metastable state during the period. Thus, the period from $t_{m\text{-}bcc}$ to t_s is the incubation period for the OOT from metastable bcc-sphere to hex-cylinder. Existence of the incubation time suggests that this OOT proceeds via the nucleation and growth process. Here, we would like to note that the slight increase of D in the incubation period is considered to indicate a signature of pre-transitional phenomenon [14].

The time evolutions of I_m, σ_q^2, and D in the OOT processes after t_s are interpreted as reported earlier in the companion paper [14]. The net scattering peak should consist of the scattering from the bcc-sphere phase and that from the hex-cylinder phase, because the bcc-sphere phase and the hex-cylinder phase coexist in the system during the nucleation and growth process. The contribution of each phase depends on volume fraction of each phase in the system, and moreover, the scattering peak from the hex-cylinder phase appears at a smaller q than that from the bcc-sphere phase. Thus, the three parameters change with time as shown in Figs. 7 and 10 and as clarified in detail elsewhere [14].

Now, we have plotted the time evolutions of D in the OOT processes again by setting $t_{m\text{-}bcc}$ at 0 s in Fig. 12(a) to discuss the quench-depth dependence of the OOT processes because the time evolution of D is a quite useful structural parameter for exploring OOT processes [14]. The reset time scale is defined as t' ($\equiv t - t_{m\text{-}bcc}$) in the figure. According to Fig. 12(b), the times, t_i' and t_m' are assessed as shown in Fig. 12(a). Here, t_i' is the incubation time, $t_i' = t_s - t_{m\text{-}bcc}$, for the OOT, which corresponds to the time (shown by the arrow in Fig. 12(a)) when D vs $\log t'$ starts deviate from the linear relationship shown by the gray line in Fig. 12(b). t_m' is the time (shown by the arrow in Fig. 12(a)) when D reaches D_m defined by $(D_i + D_f)/2$, where D_i and D_f are the D values at t_i' and t_f', respectively, and t_f' is the time when D reaches a value on the gray line in the late stage of the OOT as shown in Fig. 12(b). Furthermore, $t_{1/2}'$ is defined by the time, $t_m' - t_i'$, which is inversely related to the rate of the OOT. Then, ΔT_{OOT} dependence of t_i' and $t_{1/2}'$ together with $t_{1/2}'/t_i'$ for the OOT is summarized in Table 1, and t_i' and $t_{1/2}'$ are plotted as a function of ΔT_{OOT} in Fig. 13.

For the sake of comparison, we show ΔT_{OOT} dependence of t_i, $t_{1/2}$ and $t_{1/2}/t_i$ for the OOT from equilibrium bcc-sphere to hex-cylinder in Table 2. Here, t_i and $t_{1/2}$ for $\Delta T_{OOT} = 2$ and 3 K in Table 2 are obtained by extrapolating linear relationships between $\log t_i$ and $\Delta T_{OOT}/T_{OOT}$, and between $\log t_{1/2}$ and $\Delta T_{OOT}/T_{OOT}$, previously reported in Ref. [14], while those for $\Delta T_{OOT} = 4$ K were actually measured [14]. By comparing Tables 1 and 2, t_i' and $t_{1/2}'$ for $\Delta T_{OOT} = 2$ and 3 K are found to be almost six times of t_i and $t_{1/2}$ for $\Delta T_{OOT} = 2$ and 3 K, respectively. This indicates that the rate of the OOT is much slower for metastable bcc-sphere than that for equilibrium bcc-sphere. $t_{1/2}'/t_i'$'s for $\Delta T_{OOT} = 2$ and 3 K are a little larger than $t_{1/2}/t_i$'s for $\Delta T_{OOT} = 2$ and 3 K, respectively, but they are constant values independent of ΔT_{OOT}, implying that the OOT process is characterized by a single time scale. Though t_i', $t_{1/2}'$ and $t_{1/2}'/t_i'$ for $\Delta T_{OOT} = 4$ K are also longer than t_i, $t_{1/2}$ and $t_{1/2}/t_i$ for $\Delta T_{OOT} = 4$ K, the trend in t_i', $t_{1/2}'$ and $t_{1/2}'/t_i'$ for $\Delta T_{OOT} = 4$ K is different from that for $\Delta T_{OOT} = 2$ and 3 K. This trend can be more clearly seen in Fig. 13. The data points for $\Delta T_{OOT} = 4$ K appear to deviate from the fitting lines obtained from the data points of $\Delta T_{OOT} = 2$ and 3 K. Reflecting the deviation, t_i' and $t_{1/2}'$ for $\Delta T_{OOT} = 4$ K are larger than t_i and $t_{1/2}$ for $\Delta T_{OOT} = 4$ K only by a factor of about 2 and 4, respectively, instead of the factor of 6 found for t_i' and $t_{1/2}'$ at $\Delta T_{OOT} = 2$ and 3 K relative to t_i and $t_{1/2}$ for the same ΔT_{OOT}'s. Thus, t_i' and $t_{1/2}'$ for $\Delta T_{OOT} = 4$ K are anomalously small relative to those for $\Delta T_{OOT} = 2$ and 3 K. This is particularly so for the value, t_i'. Why metastable bcc-sphere is slowly transformed to hex-cylinder compared

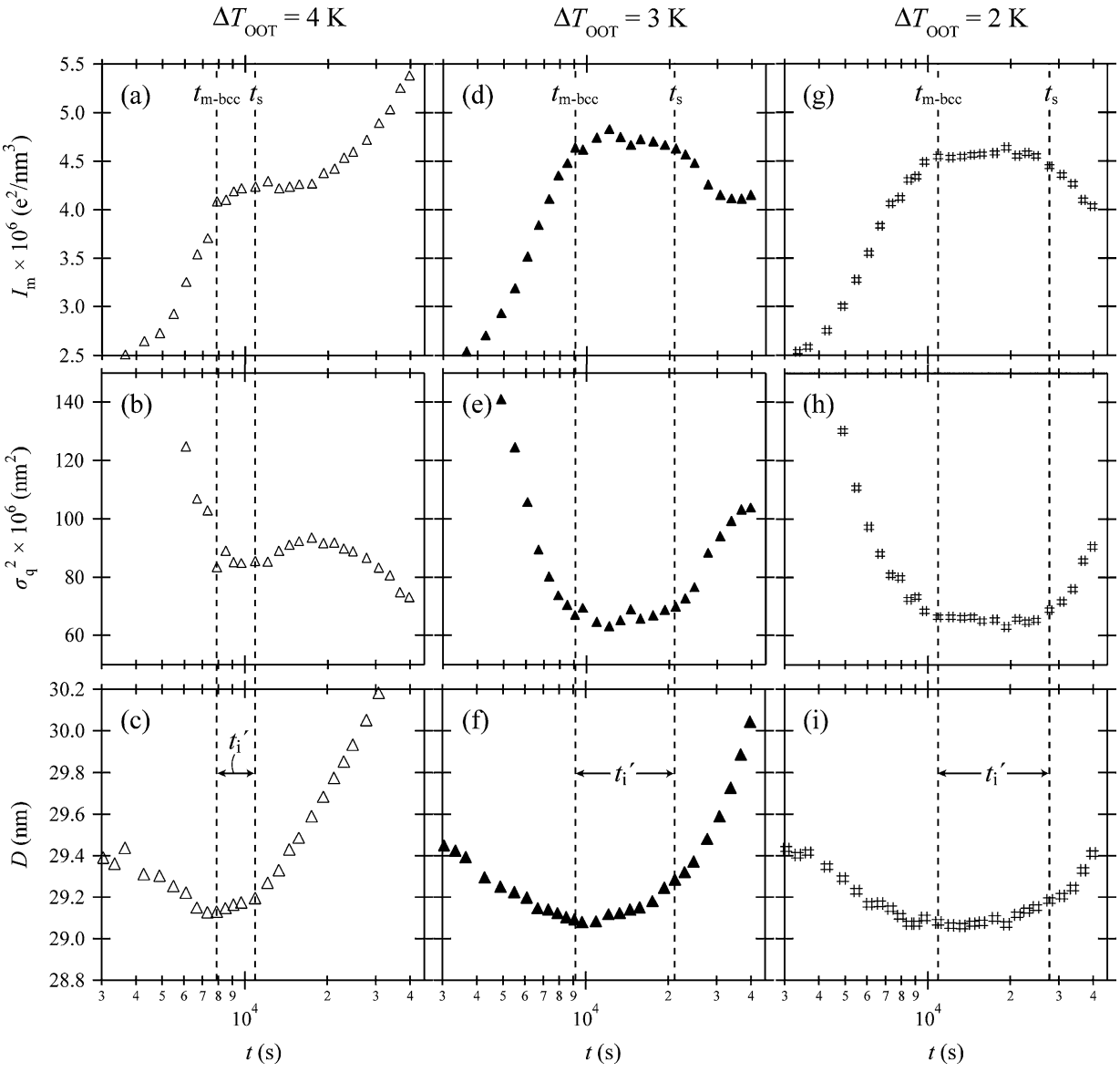

Fig. 10. Time evolutions of (a, d, g) the peak intensity, I_m, (b, e, h) the square of the half-width at half maximum, σ_q^2, (c, f, i) the Bragg spacing, D for the SIS triblock copolymer in $\Delta T_{OOT}=4$, 3 and 2 K, respectively, magnified around the period when the volume-filled metastable bcc-sphere starts to undergo the OOT into hex-cylinder. The broken lines indicate the times, $t_{m\text{-}bcc}$ and t_s, where the volume-filled metastable bcc-sphere is formed and starts to undergo the OOT, respectively. These times are characterized by the time changes of the three parameters, I_m, σ_q^2, and D.

with equilibrium bcc-sphere, and why suppression of the transformation rate for $\Delta T_{OOT}=4$ is anomalously small? To solve the puzzle, we try to analyze scaled structure factor immediately before the time, t_i', i.e. before the transformation starts.

Fig. 14 shows the scaled structure factors for (1′) $\Delta T_{OOT}=2$ K, (2′) $\Delta T_{OOT}=3$ K, and (3′) $\Delta T_{OOT}=4$ K for the OOT from metastable bcc-sphere to hex-cylinder, and (4′) $\Delta T_{OOT}=4$ K in the OOT from equilibrium bcc-sphere to hex-cylinder. In Fig. 14(b), the scaled structure factors are shifted up by one decade relative to the immediately below in order to avoid overlaps. The one numbered as (4′) indicates the actual value. By comparing these four scaled structure factors, the followings are clarified: (i) the profile number (1′) and (2′) are perfectly identical and significantly broader than the profile number (4′), which is clearly observed in the second- and third-order peak in the scaled structure factors. Therefore, the metastable bcc-sphere system is more distorted than the equilibrium bcc-sphere system, which accounts for the slower OOT rate, via the epitaxial mechanism, for the metastable bcc-sphere by a factor of about 6. (ii) The profile number (3′) has different from the profile number (1′) and (2′) in a point that the position of the third-order peak is smaller than $\sqrt{3}$. This intriguing difference or the distortion appeared in the third-order peak is not understood well at present stage. It might reflect a trigger for the anomalously fast OOT rate from metastable bcc-sphere for $\Delta T_{OOT}=4$ K compared with the OOT rate from metastable bcc-sphere for $\Delta T_{OOT}=2$ and 3 K, though the rate is still slower than the rate from equilibrium bcc-sphere for $\Delta T_{OOT}=4$ K because of this distortion.

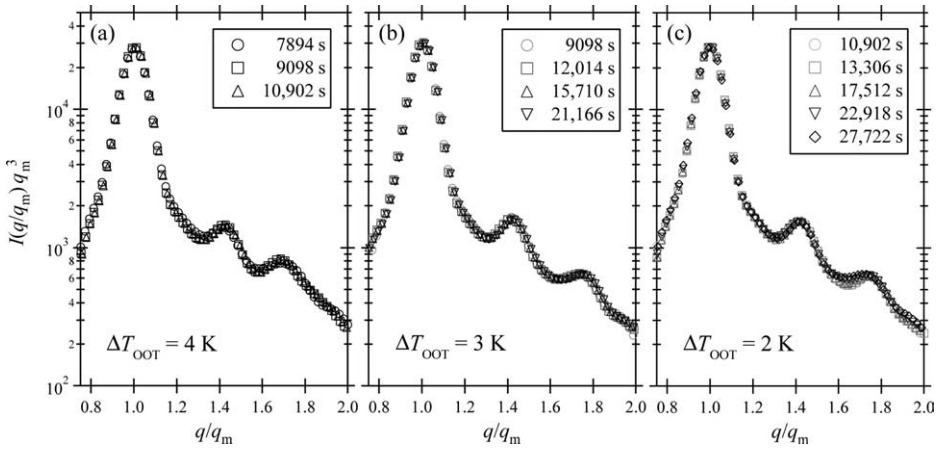

Fig. 11. Time evolutions of the scaled structure factor for metastable bcc-sphere at various times during the incubation period: ΔT_{OOT}=(a) 4, (b) 3 and (c) 2 K, shown by the plots of $I(q/q_m)q_m^3$ vs q/q_m.

4.3. Kinetic pathways of the ordering processes for the SIS triblock copolymer

So far, we have discussed the ordering processes from disorder-sphere to hex-cylinder and to bcc-sphere, and moreover, the OOT process from metastable bcc-sphere to hex-cylinder during the two-step ordering of hex-cylinder. Those results would lead us to visualize the following possible kinetic pathways. The ordering processes of the SIS triblock copolymer are found to be classified into the three kinds, the kinetic pathways of which can be illustrated in Fig. 15. Fig. 15(a) shows the ones for the single-step ordering of hex-cylinder. In the cases of the large quenches with ΔT_1 and ΔT_2 ($\Delta T_1 > \Delta T_2$), the system transforms directly from disorder-sphere with the free energy, G_d, to hex-cylinder with the free energies, G_1 and G_2 ($G_1 < G_2 < G_d$), via the free

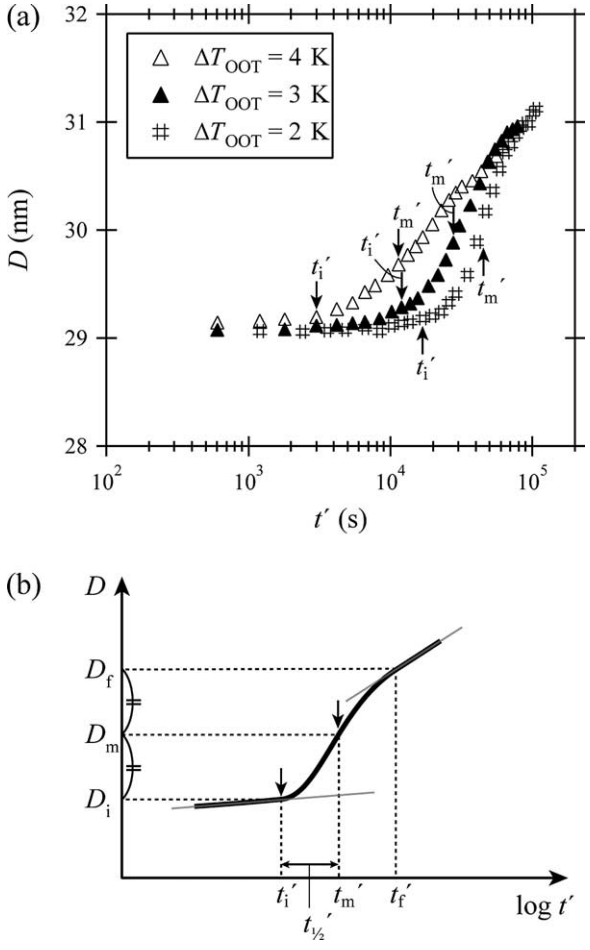

Fig. 12. (a) Replotted time evolution of Bragg spacing, D against the reset time, t' ($=t-t_{m\text{-}bcc}$), by setting $t_{m\text{-}bcc}$ at $t'=0$ s. (b) Definitions of an incubation time, t_i', and a half time, $t_{1/2}'$ in the time evolution of Bragg spacing, D for the ordering from metastable bcc-sphere to hex-cylinder.

Table 1
ΔT_{OOT} dependence of t_i', $t_{1/2}'$ and $t_{1/2}'/t_i'$ in the OOT process from metastable bcc-sphere to hex-cylinder in the two-step ordering of hex-cylinder

ΔT_{OOT} (K)	2	3	4
t_i' (s)	16 820	12 018	3008
$t_{1/2}'$ (s)	25 272	18 794	8538
$t_{1/2}'/t_i'$	1.50	1.56	2.84

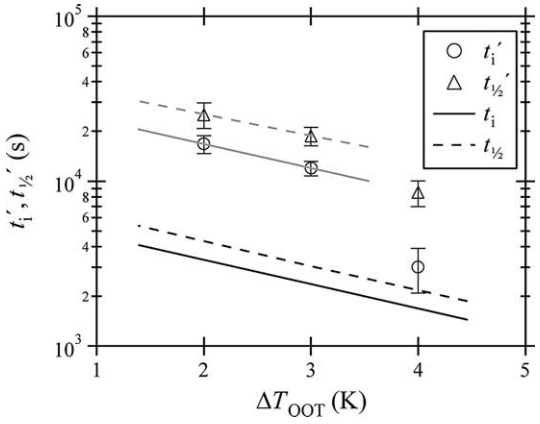

Fig. 13. ΔT_{OOT} dependence of the incubation time, t_i', and the half time, $t_{1/2}'$ in the OOT processes from metastable bcc-sphere to hex-cylinder during the two-step ordering of hex-cylinder. The gray solid line and the gray broken one, respectively, show the fitting line of t_i' and $t_{1/2}'$ obtained from the data points in ΔT_{OOT}=2 and 3 K. The corresponding results on t_i and $t_{1/2}$ from equilibrium bcc-sphere to hex-cylinder are also shown as the black solid line and the black broken one, respectively, for the sake of comparison.

Table 2
ΔT_{OOT} dependence of t_i, $t_{1/2}$ and $t_{1/2}/t_i$ in the OOT process from equilibrium bcc-sphere to hex-cylinder

ΔT_{OOT} (K)	2	3	4
t_i (s)	3356	2392	1705
$t_{1/2}$ (s)	4272	3027	2144
$t_{1/2}/t_i$	1.27	1.27	1.26

energy barriers, ΔG_1 and ΔG_2 for the observed ordering processes. The incubation time of the single-step ordering of hex-cylinder strongly depends on ΔT_{LDOT}, and the free energy barrier accordingly depends on ΔT_{LDOT} ($\Delta G_1 < \Delta G_2$), as suggested by Fig. 8(a). On the other hand, Fig. 15(b) shows the kinetic pathways for the ordering of bcc-sphere. It also proceeds via the nucleation and growth process, and the kinetic pathways can be expressed similarly to those of the single-step ordering of hex-cylinder. However, the incubation time of the ordering of bcc-sphere hardly change with ΔT_{LDOT} as shown in Fig. 8(a). Therefore, a part of the kinetic pathways are almost superposed ($\Delta G_3 \cong \Delta G_4$) even if ΔT_{LDOT}'s differ largely ($\Delta T_3 > \Delta T_4$, $G_3 < G_4$). Fig. 15(c) shows the cases for the shallow quenches ΔT_5 and ΔT_6 into the hex-cylinder phase, which revealed the kinetic pathways of the two-step ordering into hex-cylinder. In the cases of ΔT_5 and ΔT_6 ($\Delta T_5 > \Delta T_6$), the free energy barriers for the single-step ordering of hex-cylinder, ΔG_5 and ΔG_6, are expected to be larger than those for the ordering of metastable bcc-sphere, ΔG_{51} and ΔG_{61} ($\Delta G_{51} \cong \Delta G_{61}$). Therefore, the system prefers to first transform into metastable bcc-sphere with the free energy, G_{5m} and G_{6m} ($G_{5m} \cong G_{6m} < G_d$). The kinetic pathways in these cases are almost identical with those of the ordering of equilibrium bcc-sphere until the system reaches the free energy level, G_{5m} and G_{6m}. The first-step free energy barriers are nearly identical to those for equilibrium bcc-sphere ($\Delta G_{51} \cong \Delta G_{61} \cong \Delta G_3 \cong \Delta G_4$) as inferred from Fig. 8(a). After that, the kinetic pathways differ depending on ΔT_{OOT}. The OOT from metastable bcc-sphere to hex-cylinder with the free energy, G_5 and G_6 ($G_5 < G_6 < G_{5m} \cong G_{6m}$) proceeds via the nucleation and growth process, and the second-step free energy barriers, ΔG_{52} and ΔG_{62} ($\Delta G_{52} < \Delta G_{62}$), depend on ΔT_{OOT} as suggested by Fig. 13, and are larger than the first-step energy barriers, ΔG_{51} and ΔG_{61}, as inferred by comparing t_i's in Fig. 8(a) with t_i''s in Fig. 13.

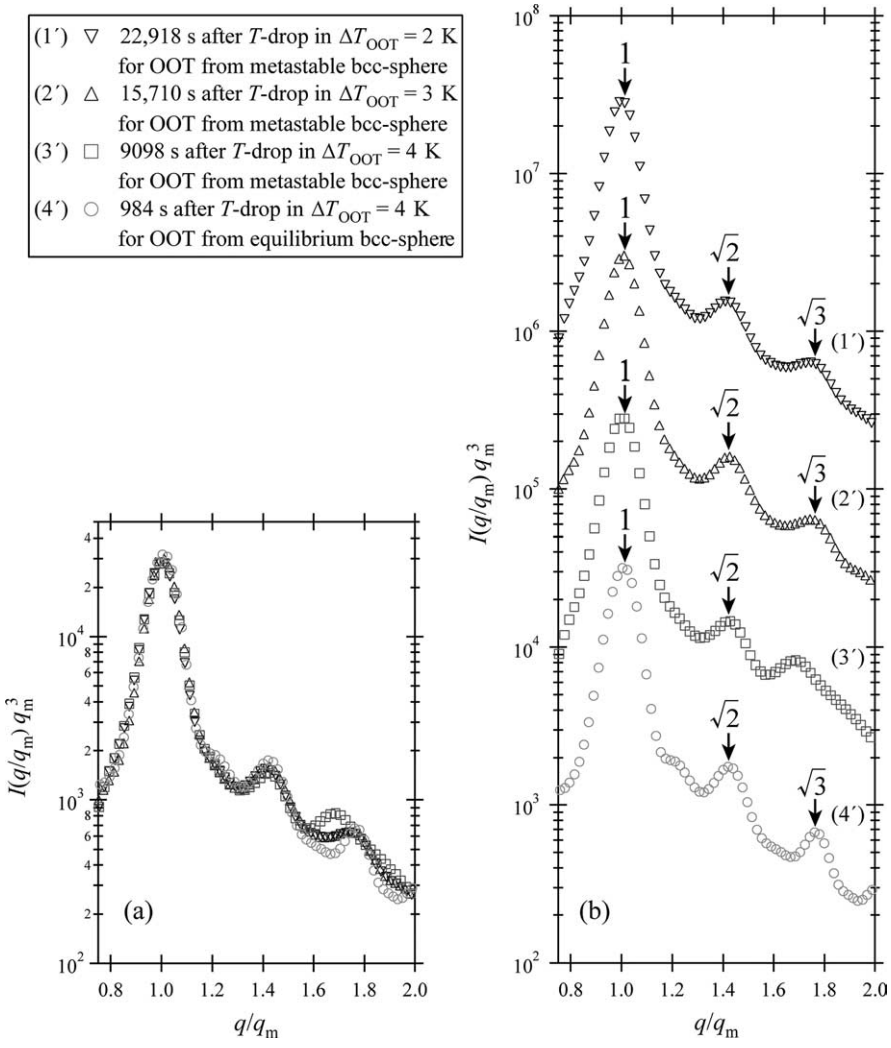

Fig. 14. Scaled structure factors for (1′) $\Delta T_{OOT} = 2$ K, for (2′) $\Delta T_{OOT} = 3$ K, and for (3′) $\Delta T_{OOT} = 4$ K immediately before the OOT from metastable bcc-sphere to hex-cylinder, and for (4′) $\Delta T_{OOT} = 4$ K immediately before the OOT from equilibrium bcc-sphere to hex-cylinder.

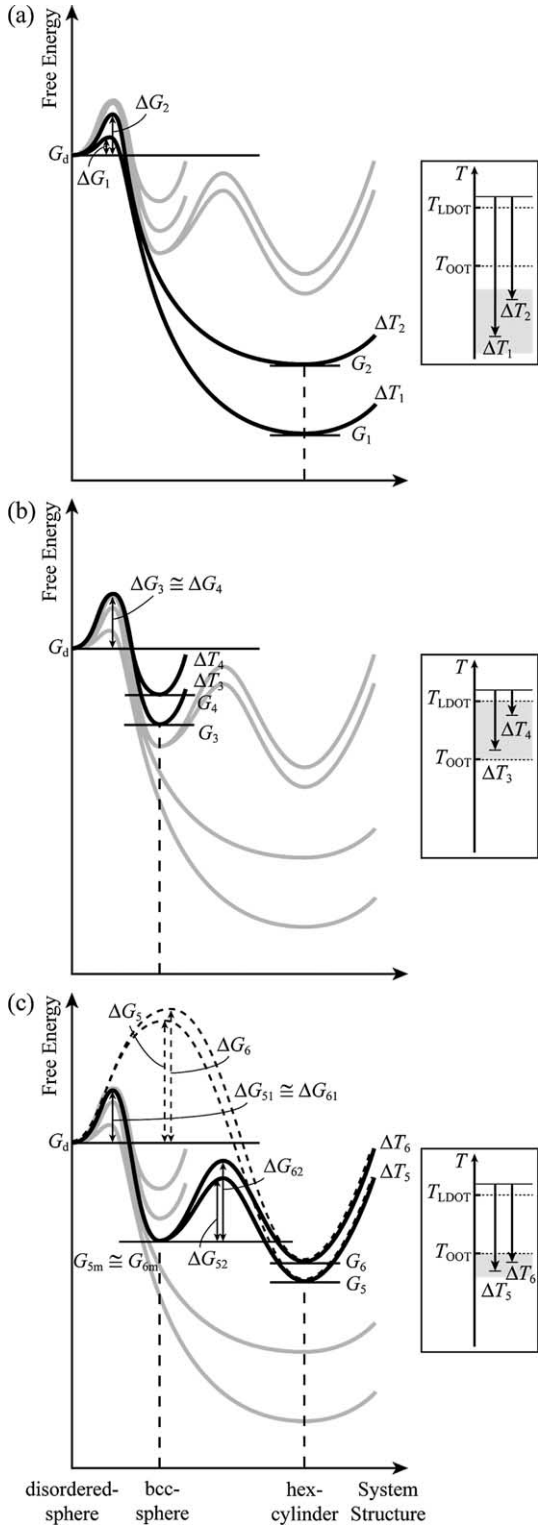

Fig. 15. Schematic illustrations showing possible kinetic pathways for the ordering processes of the SIS triblock copolymer. The gray curves shown in parts (a) to (c) were presented in order to facilitate comparisons of the kinetic pathways for the three ordering processes from disorder-sphere to (a) hex-cylinder via the single-step process, to (b) bcc-sphere, and to (c) hex-cylinder via the two-step process.

5. Concluding remarks

In this study, we have systematically explored the ordering process and kinetics of both hex-cylinder and bcc-sphere from disorder-sphere as a function of the quench depth, ΔT_{LDOT} or ΔT_{OOT}, for the SIS triblock copolymer, which exhibits the OOT between hex-cylinder and bcc-sphere, by using time-resolved SAXS. As a consequence, the ordering processes of this SIS triblock copolymer are found to be classified in the following three kinds as summarized in Scheme 1; the single step-ordering of hex-cylinder ($\Delta T_{LDOT} > 29.3$ or $\Delta T_{OOT} > 6.8$ (a-1)), the two-step ordering of hex-cylinder ($22.5 < \Delta T_{LDOT} < 29.3$ or $0 < \Delta T_{OOT} < 6.8$ (a-2) and (a-2′)), and the single-step ordering of bcc-sphere ($\Delta T_{LDOT} < 22.5$ (a-3)). The two-step ordering consists of the ordering from disorder-sphere to the volume-filled metastable bcc-sphere (a-2) and then to hex-cylinder (a-2′). The (a-2′) process is worth to be compared with the OOT process from (equilibrium) bcc-sphere to hex-cylinder (b) [14].

We found that each ordering process is characterized by the nucleation and growth process and hence characterized by the incubation time, t_i, and the half time, $t_{1/2}$ (for (a-1), (a-2), (a-3), and(b)) or by the incubation time, t_i' and the half time, $t_{1/2}'$ (for (a-2′)), where t' is the time reset to be zero when the volume-filled metastable bcc-sphere is formed, i.e. $t' \equiv t - t_{m\text{-}bcc}$, $t_{m\text{-}bcc}$ being defined in Fig. 10.

In this paper, we elucidated that the temperature range where the two-step ordering occurs, the way to evaluate the temperature range, and a possible interpretation of this intriguing phenomenon in Section 4.1.

We found that $t_{1/2}/t_i$ is constant, independent of ΔT_{LDOT} for each process studied in this work as in the case for the process (b) previously reported [14]; $t_{1/2}/t_i \cong 1.45$ for (a-1) and (a-2), 0.90 for (a-3), and 1.27 for (b) [14]. The former relationships for (a-1) to (a-3) can be extracted from Fig. 8, while the latter one for (b) from Table 2. Consequently, the nucleation and growth process can be characterized by a single time scale. As for process (a-2′), $t_{1/2}'/t_i' \cong 1.53$ for $\Delta T_{OOT} = 2$ and 3 K but 2.84 for $\Delta T_{OOT} = 4$ K (Table 1), so that it was not independent of temperature.

Comparisons between (a-2′) and (b) elucidate that $t_i' > t_i$ and $t_{1/2}' > t_{1/2}$ at a given quench depth, implying that the OOT of hex-cylinder from metastable bcc-sphere is slower than that from equilibrium bcc-sphere. This was found to be a bigger distortion for the metastable bcc-sphere system than for the equilibrium bcc-sphere system (Section 4.2 and Tables 1 and 2).

Comparisons of the process (a-1) to (a-3) under the quench depths covered in this work reveal that t_i for hex-cylinder is smaller than t_i for metastable and equilibrium bcc-sphere (Fig. 8(a)), which may be due to a greater quench for the former. t_i for metastable bcc-sphere is not smaller than but approximately equal to t_i for equilibrium bcc-sphere due to a greater distortion of metastable bcc-sphere compared to equilibrium bcc-sphere. The distortion also plays an important role for $t_{1/2}$ as seen by the fact that $t_{1/2}$ for the metastable bcc-sphere is greater than $t_{1/2}$ for the equilibrium bcc-sphere (Fig. 8(b)). A possible explanation was given by Section 4.1.

Finally, we proposed a possible kinetic pathway for each of the three ordering processes in Fig. 15.

Acknowledgements

T.H. gratefully acknowledges financial support by 21st Century COE Program for a United Approach to New Materials Science.

References

[1] Helfand E, Wasseman ZR. In: Goodman I, editor. Developments in block copolymers, vol. 1. London: Applied Science; 1982. p. 99 [chapter 4].
[2] Hashimoto T, Shibayama M, Fujimura M, Kawai H. In: Meier DJ, editor. Block copolymers, science and technology. London: Harwood Academic Publishers; 1983. p. 63.
[3] Hasegawa H, Tanaka H, Yamasaki K, Hashimoto T. Macromolecules 1987;20:1651–62.
[4] Bates FS, Fredrickson GH. In: Legge NR, Holden GR, Schroeder HE, editors. Thermoplastic elastomers. 2nd ed. Vienna: Hanser; 1996. p. 335 [chapter 12].
[5] Leibler L. Macromolecules 1980;13:1602–17.
[6] Fredrickson GH, Helfand E. J Chem Phys 1987;87:697–705.
[7] Vavasour JD, Whitmore MD. Macromolecules 1992;25:5477–86.
[8] Matsen MW, Bates FS. Macromolecules 1996;29:1091–8.
[9] Khandpur AK, Förster S, Bates FS, Hamley IW, Ryan AJ, Bras W, et al. Macromolecules 1995;28:8796–806.
[10] Sota N, Sakamoto N, Saijo K, Hashimoto T. Macromolecules 2003;36:4534–43.
[11] Sakamoto N, Hashimoto T, Han CD, Kim D, Vaidya NY. Macromolecules 1997;30:1621–32.
[12] Sakamoto N, Hashimoto T. Macromolecules 1998;31:8493–502.
[13] Kim JK, Lee HH, Ree M, Lee K-B, Park Y. Macromol Chem Phys 1998;199:641–53.
[14] Sota N, Hashimoto T. Polymer 2005;46:10392–404.
[15] Fujimura M, Hashimoto T, Kawai H. Mem Fac Eng, Kyoto Univ 1981;43:(2)224.
[16] Hashimoto T, Suehiro S, Shibayama M, Saijo K, Kawai H. Polym J 1981;13:501–16.
[17] Suehiro S, Saijo K, Ohta Y, Hashimoto T, Kawai H. Anal Chim Acta 1986;189:41–56.
[18] Hendricks RW. J Appl Crystallogr 1972;5:315–24.
[19] Sakamoto N, Hashimoto T. Macromolecules 1998;31:3292–302.
[20] Sakamoto N, Hashimoto T. Macromolecules 1998;31:3815–23.